

# The mass assembly of galaxy groups and the evolution of the magnitude gap

Ali A. Dariush<sup>\*1,2</sup>, Somak Raychaudhury<sup>1</sup>, Trevor J. Ponman<sup>1</sup>, Habib G. Khosroshahi<sup>3</sup>, Andrew J. Benson<sup>4</sup>, Richard G. Bower<sup>5</sup>, Frazer Pearce<sup>6</sup>

<sup>1</sup>*School of Physics and Astronomy, University of Birmingham, Birmingham B15 2TT, UK*

<sup>2</sup>*School of Physics and Astronomy, Cardiff University, Queens Buildings, The Parade, Cardiff, CF24 3AA, UK*

<sup>3</sup>*School of Astronomy, Institute for Research in Fundamental Sciences (IPM), P. O. Box 19395-5746, Tehran, Iran*

<sup>4</sup>*California Institute of Technology, Pasadena, CA 91125, USA,*

<sup>5</sup>*Department of Physics, University of Durham, South Road, Durham DH1 3LE, UK*

<sup>6</sup>*School of Physics and Astronomy, University of Nottingham, Nottingham, NG7 2RD, UK*

18 June 2018

## ABSTRACT

We investigate the assembly of groups and clusters of galaxies using the Millennium dark matter simulation and the associated Millennium gas simulations, and semi-analytic catalogues of galaxies. In particular, in order to find an observable quantity that could be used to identify early-formed groups, we study the development of the difference in magnitude between their brightest galaxies to assess the use of magnitude gaps as possible indicators. We select galaxy groups and clusters at redshift  $z = 1$  with dark matter halo mass  $M(R_{200}) \geq 10^{13} h^{-1} M_{\odot}$ , and trace their properties until the present time ( $z = 0$ ). Further constraints are applied to keep those galaxy systems for which the X-ray luminosity  $L_{X,\text{bol}} \geq 0.25 \times 10^{42} h^{-2} \text{erg s}^{-1}$  at redshift  $z = 0$ . While it is true that a large magnitude gap between the two brightest galaxies of a particular group often indicates that a large fraction of its mass was assembled at an early epoch, it is not a necessary condition. More than 90% of fossil groups defined on the basis of their magnitude gaps (at any epoch between  $0 < z < 1$ ) cease to be fossils within 4 Gyr, mostly because other massive galaxies are assembled within their cores, even though most of the mass in their haloes might have been assembled at early times. We show that compared to the conventional definition of fossil galaxy groups based on the magnitude gap  $\Delta m_{12} \geq 2$  (in the  $R$ -band, within  $0.5 R_{200}$  of the centre of the group), an alternative criterion  $\Delta m_{14} \geq 2.5$  (within the same radius) finds 50% more early-formed systems, and those that on average retain their fossil phase longer. However, the conventional criterion performs marginally better at finding early-formed groups at the high-mass end of groups. Nevertheless, both criteria fail to identify a majority of the early-formed systems.

**Key words:** cosmology: theory — galaxies: formation — galaxies: kinematics and dynamics — hydrodynamics — methods: numerical

## 1 INTRODUCTION

Although existing observations of the large scale structure of the Universe overwhelmingly favour cold dark matter cosmologies with hierarchical structure formation, the paradigm faces challenges both from the existence of luminous passive galaxies at high redshift, and the abundance of low-mass galaxies in the local universe (e.g. Baugh 2006; Balogh et al. 2008). Galaxies dominate the visible universe and any cosmological model is expected to reproduce the observed global properties of galaxies, at least statistically, in the first instance. A significant fraction of the evolutionary life

of many galaxies is spent in the environment of small systems (i.e. groups), where close interactions and mergers of galaxies occur with higher efficiency than in massive haloes such as galaxy clusters (e.g. Miles et al. 2004). The observable properties of the baryonic content of a group, which consists of the constituent galaxies and the inter-galactic medium (IGM), should be linked to mass assembly of the host group and its subsequent evolution. Among such observable properties, the ‘‘magnitude gap’’, i.e., the difference in the magnitudes of the two brightest galaxies, has been widely used as an optical parameter related to mass assembly of groups and clusters.

Several studies show that a system of galaxies, where most of the mass has been assembled very early, de-

\* E-mail: Ali.Dariush@astro.cf.ac.uk

velops a larger magnitude gap compared to systems that form later. The idea is supported in observational samples (e.g. Ponman et al. 1994; Khosroshahi, Jones, & Ponman 2004; Khosroshahi, Ponman, & Jones 2007), theoretical studies (e.g. Milosavljević et al. 2006; van den Bosch et al. 2007) and in detailed analysis of N-body numerical simulations (Barnes 1989; D’Onghia et al. 2005; Dariush et al. 2007). These studies also predict that such early-formed galaxy groups or clusters should be relaxed and relatively more isolated systems in comparison to their later-formed counterparts.

Jones et al. (2003) defined such early-formed systems (also known as *fossils*) to have a minimum X-ray luminosity of  $L_{X,\text{bol}} \geq 0.25 \times 10^{42} h^{-2} \text{erg s}^{-1}$ , and a large magnitude gap in the *R*-band between their first two brightest galaxies, i.e.  $\Delta m_{12} \geq 2.0$ , to distinguish them from late-formed groups and clusters. Recent research based on the Sloan Digital Sky Survey has either used only the optical criterion (Santos, Mendes de Oliveira, & Sodr e 2007) or both optical and X-ray criteria (Eigenthaler & Zeilinger 2009; Voevodkin et al. 2009; La Barbera et al. 2009) to identify fossils. In the former case, if the optical definition is solely employed, the chance of identifying truly early-formed systems diminishes, since a large fraction of the systems detected might be in the stage of collapsing for the first time, and so would not be X-ray luminous.

From numerical simulations, von Benda-Beckmann et al. (2008) found that  $\Delta m_{12}$  may not be a good indicator for identifying early-formed groups, since the condition would no longer be fulfilled when a galaxy of intermediate magnitude fell into the group. This study was based on simulations of dark matter particles only, and does not reveal how frequently such a situation would arise. Other, potentially more robust, magnitude gap criteria have been considered in the literature. For example, Sales et al. (2007) finds that the difference in magnitude between the first and  $10^{\text{th}}$  brightest galaxies in three fossil groups span a range of  $\sim 3\text{--}5$ , in agreement with their results from the analysis of the Millennium data together with the semi-analytic catalogue of Croton et al. (2006).

The overall number of observed fossil galaxy groups is small, making it difficult for observed systems to be statistically compared to simulated systems. In spite of their low space density, fossils have been used to test models of cosmological evolution (Milosavljević et al. 2006; Khosroshahi, Ponman, & Jones 2007; von Benda-Beckmann et al. 2008; D az-Gim enez, Muriel, & Mendes de Oliveira 2008), since the criteria for observationally identifying such systems are simple (Jones et al. 2003; Khosroshahi, Ponman, & Jones 2006), and it is generally assumed that they are the archetypal relaxed systems, consisting of a group-scale X-ray halo, the optical image being dominated by a giant elliptical galaxy at the core (Ponman et al. 1994). Indeed, if they are relaxed early-formed systems, fossil groups can be the ideal systems in which to study mechanisms of feedback, and the interaction of central AGN and the IGM of the group, since the effect of the AGN would not be complicated by the effect of recent mergers (Jetha et al. 2008, 2009). The lack of recent merging activity would also predict the absence of current or recent star formation in early-type galaxies belonging to fossil groups (e.g. Nolan, Raychaudhury, & Kab an 2007), and the relative dearth of red star-forming galaxies compared to similar elliptical-dominated non-fossil groups and clusters (Mahajan & Raychaudhury 2009).

The use of cosmological simulations in the study of the evolution of galaxy groups will have to employ a semi-analytic scheme for simulating galaxies, and the results will be dependent on the appropriate characterisation of the models that describe galaxy for-

mation and evolution. Once the hierarchical buildup of dark matter haloes is computed from N-body simulations, galaxy formation is modelled by considering the rate at which gas can cool within these haloes. This involves assumptions for the rate of galaxy merging (driven by dynamical friction) and the rate and efficiency of star formation and the associated feedback in individual galaxies (Croton et al. 2006; Bower et al. 2006).

In a previous paper (Dariush et al. 2007), we studied the formation of fossil groups in the Millennium Simulations, and showed that the conventional definition of fossils (namely a large magnitude gap between the two brightest galaxies within half a virial radius and a lower limit to the X-ray luminosity  $L_{X,\text{bol}} \geq 2.5 \times 10^{42} h^{-2} \text{erg s}^{-1}$ ), results in the identification of haloes which are  $\approx 10\%$ - $20\%$  more massive than the rest of the population of galaxy groups with the same halo mass and X-ray luminosity, when the Universe was half of its current age. This clearly indicates an early formation epoch for fossils. In addition, it was shown that the conventional fossil selection criteria filter out spurious systems, and therefore there is a very small probability for a large magnitude gap in a halo to occur at random. The fraction of late-formed systems that are spuriously identified as fossils was found to be  $\approx 4\text{--}8\%$ , almost independent of halo mass (Dariush et al. 2007; Smith et al. 2010). Another important outcome of the Dariush et al. (2007) study was the consistency between the space density of fossils found in the simulations and that from observational samples.

Although the results from this previous analysis of the Millennium simulations are shown to be in fair agreement with observation, we did not investigate the evolution of the magnitude gap in either fossil or control groups with redshift. Furthermore, the number of (fossil or control) groups used was small ( $\sim 400$ ), which did not allow us to fully explore the connection between the halo mass and magnitude gap in such systems.

In this paper, we select early-formed galaxy groups from the Millennium simulations, purely on the basis of their halo mass evolution from present time up to redshift  $z \approx 1.0$ , and, with the help of associated semi-analytic catalogues, study the evolution of the magnitude gap between their brightest galaxies. Our aim is to (a) investigate how well the conventional optical selection criterion, namely the  $\Delta m \geq 2$  gap between the two brightest galaxies, is able to identify early-formed galaxy groups, and (b) to find whether we can find a better criterion to identify groups that have assembled most of their mass at an early epoch.

In §2, we describe the various simulation suites used in this work, and in §3 the data we extract from them. In §4, we study in detail the evolution with epoch of various measurable parameters for a large sample of early-formed “fossil systems” and two comparable sample of control systems, and compare these properties. In §5, we examine the case for a revision of the criteria to observationally find fossil in order to ensure a higher incidence of genuine early-formed systems. We summarise our conclusions in §6. We adopt  $H_0 = 100 h \text{ km s}^{-1} \text{ Mpc}^{-1}$  for the Hubble constant, with  $h = 0.73$ .

## 2 DESCRIPTION OF THE SIMULATIONS

### 2.1 The Millennium Simulation

The Millennium Run consists of a simulation, in a Universe consistent with concordance  $\Lambda$ CDM cosmology, of  $2160^3$  particles of individual mass  $8.6 \times 10^8 h^{-1} M_\odot$ , within a co-moving periodic box of side  $500 h^{-1} \text{ Mpc}$ , employing a gravitational softening of

$5h^{-1}$  kpc, from redshift  $z = 127$  to the present day (Springel et al. 2005). The basic setup is that of an inflationary Universe, dominated by dark matter particles, leading to a bottom-up hierarchy of structure formation, which involves the collapse and merger of small dense haloes at high redshifts, into the modern-day observed large virialised systems such as groups and clusters. The cosmological parameters used by the Millennium Simulation were  $\Omega_\Lambda = 0.75$ ,  $\Omega_M = 0.25$ ,  $\Omega_b = 0.045$ ,  $n = 1$ , and  $\sigma_8 = 0.9$ , and the Hubble parameter  $h = 0.73$ .

Dark matter haloes are found in this simulation down to a resolution limit of 20 particles, yielding a minimum halo mass of  $1.72 \times 10^{10} h^{-1} M_\odot$ . Haloes in the simulation are found using a friends-of-friends (FOF) group finder, configured to extract haloes with overdensities of at least 200 relative to the critical density (Springel et al. 2005). Within a FOF halo, substructures or subhaloes are identified using the SUBFIND algorithm developed by Springel et al. (2001), and the treatment of the orbital decay of satellites is described in the next section.

During the Millennium Simulation, 64 time-slices of the locations and velocities of all the particles were stored, spread approximately logarithmically in time between  $z = 127$  and  $z = 0$ . From these time-slices, merger trees were built by combining the tables of all haloes found at any given output epoch, thus enabling us to trace the growth of haloes and their subhaloes through time within the simulation.

## 2.2 Semi-analytic galaxy catalogues

### 2.2.1 The Croton et al. semi-analytic catalogue

Croton et al. (2006) simulated the growth of galaxies, and their central supermassive black holes, by self-consistently implementing semi-analytic models of galaxies on the dark matter haloes of the Springel et al. (2005) simulation. Their semi-analytic catalogue contains 9 million galaxies at  $z = 0$  brighter than absolute magnitude  $M_R - 5 \log h = -16.6$ , “observed” in  $B$ ,  $V$ ,  $R$ ,  $I$  and  $K$  filters. The models focus on the growth of black holes and AGN as sources of feedback sources. The inclusion of AGN feedback in the semi-analytic model (allowing central cooling to be suppressed in massive haloes that undergo quasi-static cooling), and its good agreement with the observed galaxy luminosity function, distribution of galaxy colours and of the clustering properties of galaxies, make this catalogue suitable for our study.

In this semi-analytic formulation, galaxies initially form within small dark matter haloes. Such a halo may fall into a larger halo as the simulation evolves. The “galaxy” within this halo then becomes a satellite galaxy within the main halo, and follows the track of its original dark matter halo (now a subhalo), until the mass of the subhalo drops below  $1.72 \times 10^{10} h^{-1} M_\odot$ . This limit corresponds to the 20-particle limit for dark haloes in the original Millennium Simulation. At this point the galaxy is assumed to spiral into the centre of the halo, on some fraction of the dynamical friction timescale, where it merges with the central galaxy of the larger halo (Croton et al. 2006).

### 2.2.2 The Bower et al. semi-analytic catalogue

The Bower et al. (2006) model also makes use of the Millennium Simulation, but utilises merger trees constructed with the algorithm described by Harker et al. (2007). The cooling of gas and the subsequent formation of galaxies and black holes is followed through

the merging hierarchy of each tree utilising the GALFORM semi-analytic model (Cole et al. 2000; Bower et al. 2006; Malbon et al. 2007). At  $z = 0$  this results in 4,491,139 galaxies brighter than a limiting absolute magnitude of  $M_K - 5 \log h = -19.4$ .

In addition to feedback from supernovae, the Bower et al. (2006) model accounts for energy input from AGN, resulting in a suppression of cooling in the hot atmospheres of massive haloes. The resulting galaxy population is in excellent agreement with the observed  $z = 0$  galaxy luminosity function in  $B$  and  $K$  bands, the  $z = 0$  colour distribution and also with the evolution of the galaxy stellar mass function from  $z = 0$  to  $z \approx 5$ . This model is therefore similarly well-suited to our study of fossil systems. If a halo in a merger tree has multiple progenitors, all but the most massive are considered to become subhaloes orbiting within the larger host halo and any galaxies they contain therefore become satellite galaxies in that halo.

Due to the limited resolution of the Millennium Simulation (which may cause dynamical friction timescales to be poorly estimated), the time between becoming a satellite and merging with the central galaxy of the halo is computed from the analytic dynamical friction timescale. Specifically, each new satellite is randomly assigned orbital parameters from a distribution measured from N-body simulations and the appropriate dynamical friction timescale computed following the approach of Cole et al. (2000), but multiplied by a factor of 1.5. This was found to produce the best fit to the luminosity function in Bower et al. (2006) but is also in good agreement with the results of Boylan-Kolchin, Ma & Quataert (2008) who compared the predictions of analytic dynamical friction timescales with those from idealised N-body simulations. The satellite is allowed to orbit for the period of time calculated above, after which it is merged with the central galaxy of the halo. If the host halo doubles in mass before a satellite can merge, the satellite orbit is assumed to be reset by the merging which lead to that mass growth and so a new set of orbital parameters are assigned and a new merging timescale computed.

## 2.3 The Millennium Gas Simulations

The Millennium Gas Simulations are a series of hydrodynamical models constructed within the same volume, and values of initial perturbation amplitudes and phases, as the parent dark-matter-only Millennium Simulation (see, e.g., Hartley et al. 2008). Of the three principal models completed in this work, each contains additional baryonic physics: (i) the first does not follow the effects of radiative cooling and so overpredicts the luminosities of group-scale objects significantly, (ii) the second includes a simple preheating scheme that is tuned to match the observed X-ray properties of clusters at the present day and (iii) the third includes a simple feedback model that matches the observed properties of clusters today. We have used the second of these models in this work, as we only utilise the hydrodynamical properties of the groups at  $z = 0$ , where the observational and simulation results are well matched.

The Millennium Gas Simulations consist of  $5 \times 10^8$  particles of each species, resulting in a dark matter mass of  $1.422 \times 10^{10} h^{-1} M_\odot$  per particle and a gas mass of  $3.12 \times 10^9 h^{-1} M_\odot$  per particle. The Millennium Simulation has roughly 20 times better mass resolution than this and so some perturbation of the dark matter halo locations is to be expected. In practice the position and mass of dark matter haloes above  $10^{13} h^{-1} M_\odot$  are recovered to within  $50 h^{-1}$  kpc between the two volumes, allowing straightforward halo-halo matching in the large majority of cases.

The Millennium gas simulations used exactly the same cosmo-

logical parameters as those of the dark matter simulations. With the inclusion of a gaseous component, additional care needs to be taken in choosing the gravitational softening length in order to avoid spurious heating (Steinmetz & White 1997). We use a comoving value of  $25(1+z)h^{-1}$  kpc, roughly 4% of the mean inter-particle separation (Borgani et al. 2006) until  $z = 3$ , above which a maximum comoving value of  $100h^{-1}$  kpc is adopted. A different output strategy is followed in the Millennium Gas Simulations, where the results are output uniformly in time with an interval roughly corresponding to the dynamical time of objects of interest. This strategy results in 160 rather than 64 outputs and places particular emphasis on the late stages of the simulation.

### 3 DATASETS USED IN THIS WORK

We start with a catalogue of groups extracted by the friends-of-friends (FoF) algorithm employed in the Millennium Dark matter runs. Hereafter a “group” or “group halo” would refer to a group taken from this catalogue. In order to follow the evolution of groups from  $z \sim 1$  to the present epoch, we have to combine various sets of information from this FoF group catalogue and the associated semi-analytic catalogues of galaxies, as well as the gas simulations.

We select all groups of  $M(R_{200}) \geq 10^{13} h^{-1} M_{\odot}$  from the FoF group catalogue at  $z = 0.998$ . The mass cut-off is intended to ensure that the progenitors of the present day galaxy groups are indeed groups at  $z \sim 1$  with at least four or five members (galaxies), above the magnitude cut of the catalogue. The evolution of each group was followed from  $z = 0.998$  to  $z = 0$  (at 23 discrete values, equally spaced in  $\log z$ ) by matching the position of each halo to its descendants at later redshifts.

The position of the central galaxy of each galaxy group, and the corresponding dark matter halo, were used to identify the member galaxies of each group. At each redshift and for each group halo, optical properties were extracted for its corresponding galaxies from the semi-analytic galaxy catalogue. The model galaxies become incomplete below a magnitude limit of  $M_K - 5 \log(h) \sim -19.7$ , due to the limited mass resolution of the Millennium simulation. We applied a  $K$ -band absolute magnitude cut-off of  $M_K \lesssim -19$  on galaxies at all redshifts. During the matching process, for more than 99% of the groups at each redshift, corresponding galaxies were found in the semi-analytic galaxy catalogue. The remaining groups were excluded from our final compiled list.

In order to find the gas properties of all groups at  $z = 0$ , we cross-correlated our list of groups with the Millennium gas catalogue, and find the bolometric X-ray luminosity of our selected groups at  $z=0$ .

Out of 19066 dark matter group haloes with  $M(R_{200}) \geq 10^{13} h^{-1} M_{\odot}$  selected at  $z = 0.998$ , optical properties from the semi-analytic catalogue (as well as gas properties from the gas simulations at  $z=0$ ) and the entire history of evolution at all redshifts up to  $z=0$ , were found for 17866 ( $\sim 94\%$  of the initial sample at  $z \sim 1$ ) of group haloes. Fig. 1 shows the bolometric X-ray luminosity from the Millennium gas simulation, plotted against the corresponding dark matter halo mass of each group, at redshift  $z=0$  for all of the matched 17866 groups.

The vertical dashed line in Fig. 1 corresponds to the conventional X-ray luminosity threshold ( $L_{X,\text{bol}} = 0.25 \times 10^{42} h^{-2} \text{erg s}^{-1}$ ) for fossil groups (Jones et al. 2003), as adopted in Sec. 4.2.1 to define X-ray bright groups. There are 14628 groups above this threshold, out of 17866 groups. These X-ray bright groups will constitute the main data set for the rest of our analysis, except for §4.1

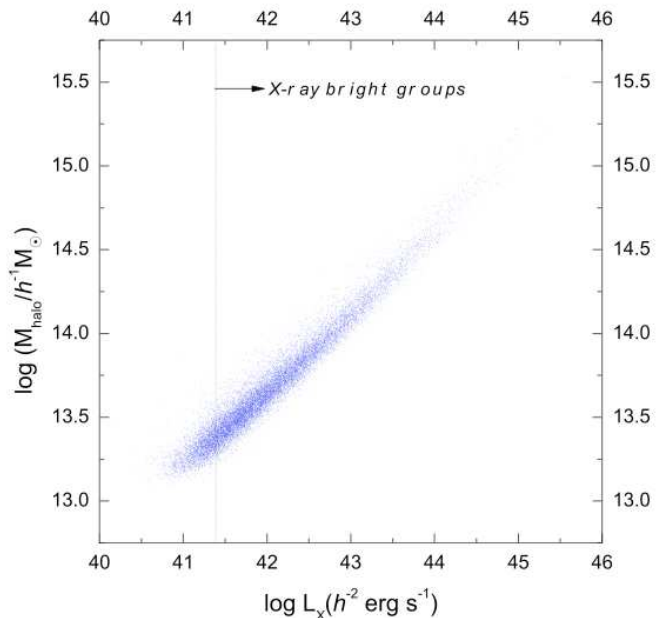


**Figure 1.** The relation between the mass of group haloes (within  $R_{200}$ ) at  $z = 0$  from the Millennium DM simulation, and the bolometric X-ray luminosity of the corresponding haloes in the Millennium gas simulation. All groups have  $M(R_{200}) \geq 10^{13} h^{-1} M_{\odot}$  at  $z \sim 1.0$ . The vertical dashed-line corresponds to the X-ray luminosity threshold  $L_{X,\text{bol}} = 0.25 \times 10^{42} h^{-2} \text{erg s}^{-1}$  generally adopted to define fossil groups (see Sec. 4.2.1). Of the 17866 groups matched in the two catalogues, 14628 groups lie above this threshold. In this paper, we call these “X-ray bright groups”.

and §5.3, where the whole range of halo mass will be explored to study the magnitude gap statistics and the local environment of groups,

## 4 RESULTS

### 4.1 The $R$ -band Magnitude Gap Statistic

The dynamical friction  $f_{\text{dyn}}$  will cause the more luminous galaxies in a group to merge on a time scale which depends upon the velocity dispersion of the group, and since  $f_{\text{dyn}} \propto v^{-2}$  this is more frequent in poorer groups than in clusters (e.g. Miles et al. 2004, 2006). As a result, on group scales, the likelihood of a few of the brightest galaxies merging to form the brightest galaxy, leading to a large magnitude gap within a Hubble time, is higher. Thus, the distribution of the magnitude gap between the brightest galaxy, and the second and third brightest galaxies, in each group, is often used as an indicator the dynamical age of group, particularly in fossil groups (Milosavljević et al. 2006; van den Bosch et al. 2007; Dariush et al. 2007; von Benda-Beckmann et al. 2008).

We determine the magnitude gaps from the Millennium semi-analytic models of Bower et al. (2006) and Croton et al. (2006), and compare them with observational results from the Sloan Digital Sky Survey (SDSS) C4 cluster catalogue data of Miller et al. (2005) and the 2-degree Field Galaxy Redshift Survey (2dFGRS) group catalogue of van den Bosch et al. (2007).

The 2dFGRS group catalogue is constructed based on a halo-based group finder algorithm of Yang et al. (2005) and contains

$\sim 6300$  groups within the mass range  $\log(M/h^{-1} M_{\odot}) \geq 13.0$  where the mass of each group has been determined from the total luminosity of all group members brighter than  $M_{b_j} - 5 \log h = -18$ . The C4 catalogue Miller et al. (2005) consists of  $\sim 730$  clusters identified in the spectroscopic sample of the Second Data Release (DR2) of the SDSS inside the mass range  $13.69 \leq \log(M/h^{-1} M_{\odot}) \leq 15.0$ , estimated from the total  $r$ -band optical luminosity of cluster galaxies.

The results of the comparison between our distribution of the estimated  $R$ -band magnitude gaps from semi-analytic models of Bower et al. (2006) as well as Croton et al. (2006), based on the Millennium simulation (red triangles and black circles respectively), and the observed results from the C4 cluster catalogue and the 2dFGRS group catalogues (blue histogram), are shown in Fig. 2. The magnitude gap statistics  $\Delta m_{12}$  and  $\Delta m_{13}$  from Bower et al. (2006) are in excellent agreement with those obtained from 2dFGRS group catalogue and SDSS C4 catalogue of clusters. However, the semi-analytic galaxy catalogue of Croton et al. (2006) predicts a larger fraction of groups with  $\Delta m_{12} \geq 2.0$  for both the SDSS and 2dFGRS samples. This is in particular of great importance to the determination of the space density of fossil galaxy groups, and the comparison of fossil samples drawn from simulated and observed catalogues, which use the magnitude gap as a key discriminant, (e.g., see Table 1 of Dariush et al. 2007).

The shift of the distribution of  $\Delta m_{12}$  and  $\Delta m_{13}$  to larger values than observed in the Croton et al. (2006) model may reflect the fact that in the Bower et al. (2006) model, the treatment of dynamical friction differs from that used by Croton et al. (2006). In both models, N-body dynamics are used to follow the orbital decay of satellite galaxies whose subhalo can be resolved. However, when the subhalo can no longer be reliably followed, the dynamical friction calculations differ. In the Bower et al. (2006) model, the dynamical friction timescale is initially calculated following Cole et al. (2000). However, if the host halo of the satellite is deemed to undergo a formation event (corresponding to a mass doubling since the previous formation event), before the satellite merges, then a new orbit for the satellite is selected at random, and the dynamical friction timescale for the satellite is recalculated. This calculation takes into account the scattering of galaxies to larger energy orbits during the merger of their parent halo.

Another possible cause for the success of the Bower et al. (2006) model in matching the magnitude gap statistics is that it predicts a large scatter in the relation between galaxy stellar mass and halo mass—significantly more than in the Croton et al. (2006) model. As a result, sometimes rather large satellite haloes arrive carrying relatively small galaxies resulting in a large difference between the magnitude of the dominant object and the next most luminous. This difference occurs because the AGN feedback is not guaranteed to switch off the cooling at a particular halo mass in the Bower et al. (2006) model, as it depends on the merging and cooling history of each halo.

For the purposes of this work, the fact that the Bower et al. (2006) method for computing merging timescales results in good agreement with the observed magnitude gap distributions, makes it well suited for the remainder of our study.

## 4.2 Evolution of galaxy groups

In cosmological simulations, the age of galaxy groups can be expressed in terms of the rate of the mass assembly of the groups. This means that for a given group halo mass, groups that formed early, assemble most of their masses at an earlier epoch in comparison to

younger groups. Thus the *assembly time* of a dark matter halo, defined as the look-back time at which its main progenitor reaches a mass that is half of the halo’s present day mass, is larger in “older” systems than in “younger” ones. Of course, in cosmological simulations such as the Millennium runs, where the structures in Universe form hierarchically, massive systems which form later turn out to have shorter assembly time than low mass groups. Therefore one should take into account the mass of systems when comparing the mass assembly of various types of groups and clusters.

### 4.2.1 Fossil groups of galaxies

How is the history of mass assembly of a group or cluster related to its present observable parameters? It is expected that groups which have formed earlier tend to be more dynamically relaxed, thus resulting in a hotter intergalactic medium (IGM) and being more likely to be X-ray luminous (Miles et al. 2004; Forbes et al. 2006). It has been shown that in X-ray luminous systems, the brightest galaxies are bigger and more optically luminous and those belonging to systems that have little or no diffuse X-ray emission (e.g., Khosroshahi et al. 2004). On the other hand, groups with the same mass that have formed late, and are still in a state of collapse, would not show X-ray emission associated with their IGM (Rasmussen et al. 2006; Bai et al. 2010), and are less likely to be dominated by a massive elliptical in their cores.

Hitherto the so-called *fossil galaxy groups*, which are supposed to be canonical examples of groups that have formed early, have been identified by requiring that their X-ray luminosities exceed  $L_{X,\text{bol}} \geq 0.25 \times 10^{42} h^{-2} \text{erg s}^{-1}$  (e.g. Khosroshahi, Ponman, & Jones 2007; Jones et al. 2003). In addition, a fossil group needs to have, within half a virial radius of the group’s centre, the second brightest galaxy to be at least 2-mag fainter than the brightest galaxy, i.e.  $\Delta m_{12} \geq 2.0$ <sup>1</sup>. So far these two observational criteria have been jointly used to explore fossil groups and clusters of galaxies. Therefore, Fig. 3, which displays all the *X-ray bright groups* fulfilling the X-ray criterion in Fig. 1, and the optical criterion  $\Delta m_{12} \geq 2.0$  (dotted horizontal line) should separate groups which have been formed earlier in comparison to their counterparts with  $\Delta m_{12} < 2.0$ .

Note that, in numerical simulations, fossils are identified as groups with  $\Delta m_{12} \geq 2.0$  within  $R_{200}$  or  $0.5R_{200}$ . Our results from this study as well as those represented in Dariush et al. (2007) show that the fraction of fossils (and therefore their space densities) depend on the search radius within which  $\Delta m_{12}$  is estimated, whereas the history or mass assembly does not change that much.

### 4.2.2 The mass assembly of X-ray fossil groups

Let us introduce the parameter  $\alpha_z$  which for an individual group is the ratio of its mass at redshift  $z$  to its final mass at  $z = 0$ , i.e.  $\alpha_z \equiv M_z/M_{z=0}$ . Thus at a given redshift  $z$ , groups with larger  $\alpha_z$  have assembled a larger fraction of their final mass by  $z$  than groups with smaller values of  $\alpha_z$ .

In Fig. 3, we plot the magnitude gap  $\Delta m_{12}$  (within  $0.5R_{200}$ ), estimated for all 14628 X-ray bright groups (i.e. groups with  $L_{X,\text{bol}} \geq 0.25 \times 10^{42} h^{-2} \text{erg s}^{-1}$ ) at  $z = 0$  as a function of their mass fraction  $\alpha_{1,0}$  at  $z = 1$ . Groups are colour-coded according to their dark matter halo mass. The horizontal dashed line separates

<sup>1</sup> This condition can be replaced by  $\log(L_2/L_1) \leq -0.8$  where  $L_1$  and  $L_2$  are the luminosities of the first two brightest galaxies.

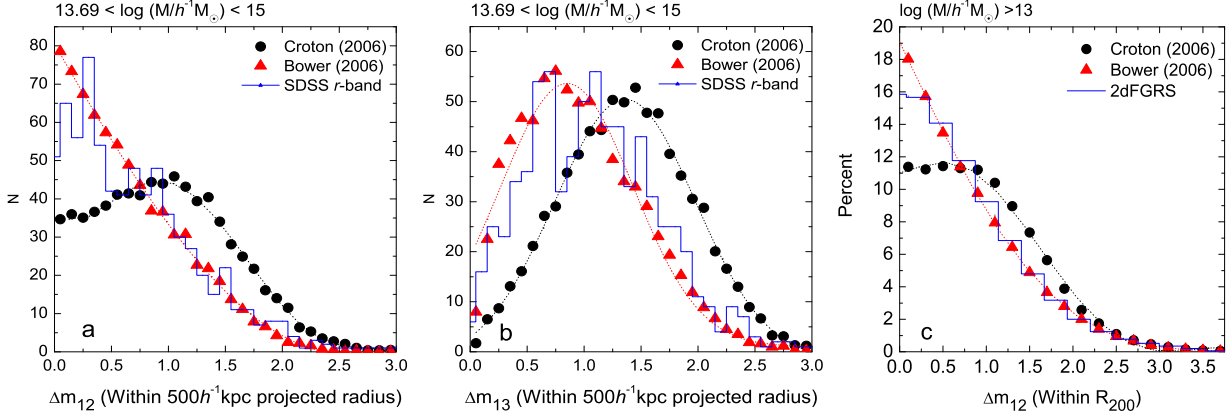


**Figure 2.** The  $R$ -band magnitude gap distribution for haloes from the Millennium semi-analytic models of Bower et al. (2006) (*red triangles*) and Croton et al. (2006) (*black circles*) superposed on the data from 2dFGRS group catalogue of van den Bosch et al. (2007) as well as SDSS C4 cluster catalogue of Miller et al. (2005) (*blue histograms*). (a) The magnitude gap  $\Delta m_{12}$  between the the first and second most luminous galaxies, compared with galaxies from the SDSS C4 catalogue of clusters computed within projected radius of  $500h^{-1}\text{kpc}$ . (b) The same as in (a) but for the magnitude gap  $\Delta m_{13}$  between the first and the third most luminous galaxies. (c) The magnitude gap  $\Delta m_{12}$  estimated within  $R_{200}$ , compared with galaxies from the 2dFGRS group catalogue. The  $\sim 6300$  2dFGRS groups are within the mass range  $\log(M(R_{200})/h^{-1}M_{\odot}) \geq 13.0$ , and those from SDSS C4 catalogue consist of  $\sim 730$  clusters within mass range  $13.69 \leq \log(M(R_{200})/h^{-1}M_{\odot}) \leq 15.0$ .

groups into fossils ( $\Delta m_{12} \geq 2.0$ ) and non-fossils ( $\Delta m_{12} < 2.0$ ). All data points on the right side of the *vertical dashed-line* have assembled more than 50% of their mass by  $z \sim 1.0$  and hence have a minimum assembly time of about  $\sim 7.7$  Gyr. The contour lines represent the number of data points (groups) in each of  $25 \times 25$  cells of an overlaid grid which is equally spaced along both the horizontal and vertical axes.

Three results emerge from this plot: (i) As is expected, on average the rate of mass growth in massive systems is higher than in low mass groups as the majority of massive groups and clusters have assembled less than 50% of their final mass at  $z \sim 1.0$ . (ii) Less massive groups (and therefore early-formed ones) tend to develop larger magnitude gaps in comparison to massive groups and clusters. Consequently the fraction of massive fossils, identified in this way, is less than low mass fossil groups. (iii) For any given  $\alpha_{1.0} \gtrsim 0.5$ , the majority of groups have magnitude gaps  $\Delta m_{12} \lesssim 2.0$ , as is evident from the density of contours. In other words, the number of early-formed groups with values of  $\Delta m_{12} < 2.0$  exceeds the number of fossil groups with  $\Delta m_{12} \gtrsim 2.0$ .

Unlike the first two results, the third conclusion is not in agreement with our current view that early-formed groups necessarily develop larger magnitude gaps. Clearly, the majority of groups with similar values of  $\alpha_{1.0} \gtrsim 0.5$  have smaller magnitude gaps. Without doubt, the parameter  $\Delta m_{12}$  is influenced by the infall and merging of galaxies and sub-groups within galaxy groups. This could result in the increase (in case of merging) or decrease (in case of the infalling of new galaxies) in  $\Delta m_{12}$ . Indeed, in the work of von Benda-Beckmann et al. (2008), one finds that the ‘‘fossil’’ phase of any fossil group is transient, since the magnitude gap criterion will sooner or later be violated by a galaxy comparable to the brightest galaxy falling into the core of the group.

To quantify the above results, we study the evolution with redshift of various physical parameters for two different sample of groups, drawn from the distribution of galaxy groups in Fig. 3. In the first sample, haloes are divided into **old** ( $\alpha_{1.0} \geq 0.5$ ,  $b + c$  in Fig. 3) and **young** ( $\alpha_{1.0} \leq 0.5$ ,  $a + d$  in Fig. 3) groups respectively. In the second population, haloes are classified as **X-ray fossil** ( $\Delta m_{12} \geq 2.0$ ,  $a + b$  in Fig. 3) and **control** ( $\Delta m_{12} \leq 0.5$ ,  $c + d$  in Fig. 3) groups based on the magnitude gap between the first and the second brightest galaxies within half a virial radius of the centre of the group.

For each sample, the evolution of various parameters are shown in two panels of Fig. 4. From top to bottom these parameters are:

- $\alpha_z$ , i.e. the ratio of the group halo mass at redshift  $z$  to its mass at  $z = 0$ ,
- $\Delta m_{12}$  within  $0.5R_{200}$ ,
- Ratio of the number of galaxies within  $0.5R_{200}$  at redshift  $z$  of a given galaxy group to the number of galaxies within  $0.5R_{200}$  at redshift  $z = 0$  of the same group, i.e.  $G_z$ ,
- Group velocity dispersion  $\sigma_V$  in  $\text{km s}^{-1}$ .

In each panel of Fig. 4, the left, middle, and right columns correspond to different ranges in group mass, as indicated. The left panel in Fig. 4 illustrates X-ray fossil (*red triangles*) and control (*blue circles*) groups respectively while the right panel shows old (*red stars*) and young (*blue squares*) groups. The horizontal *green dashed-lines* intersect y-axes at  $G_z = 1$ . Errors on data points are the standard error on the mean, i.e.  $\sigma/\sqrt{N}$ , where  $\sigma$  is the standard deviation of the original distribution and  $N$  is the sample size.

A comparison between Figs. 4a1, a2, a3 and Figs. 4a4, a5, a6 shows that older groups, which have been picked up according to their lower rate of mass growth (i.e. larger  $\alpha_{1.0}$ ), represent a *per-*

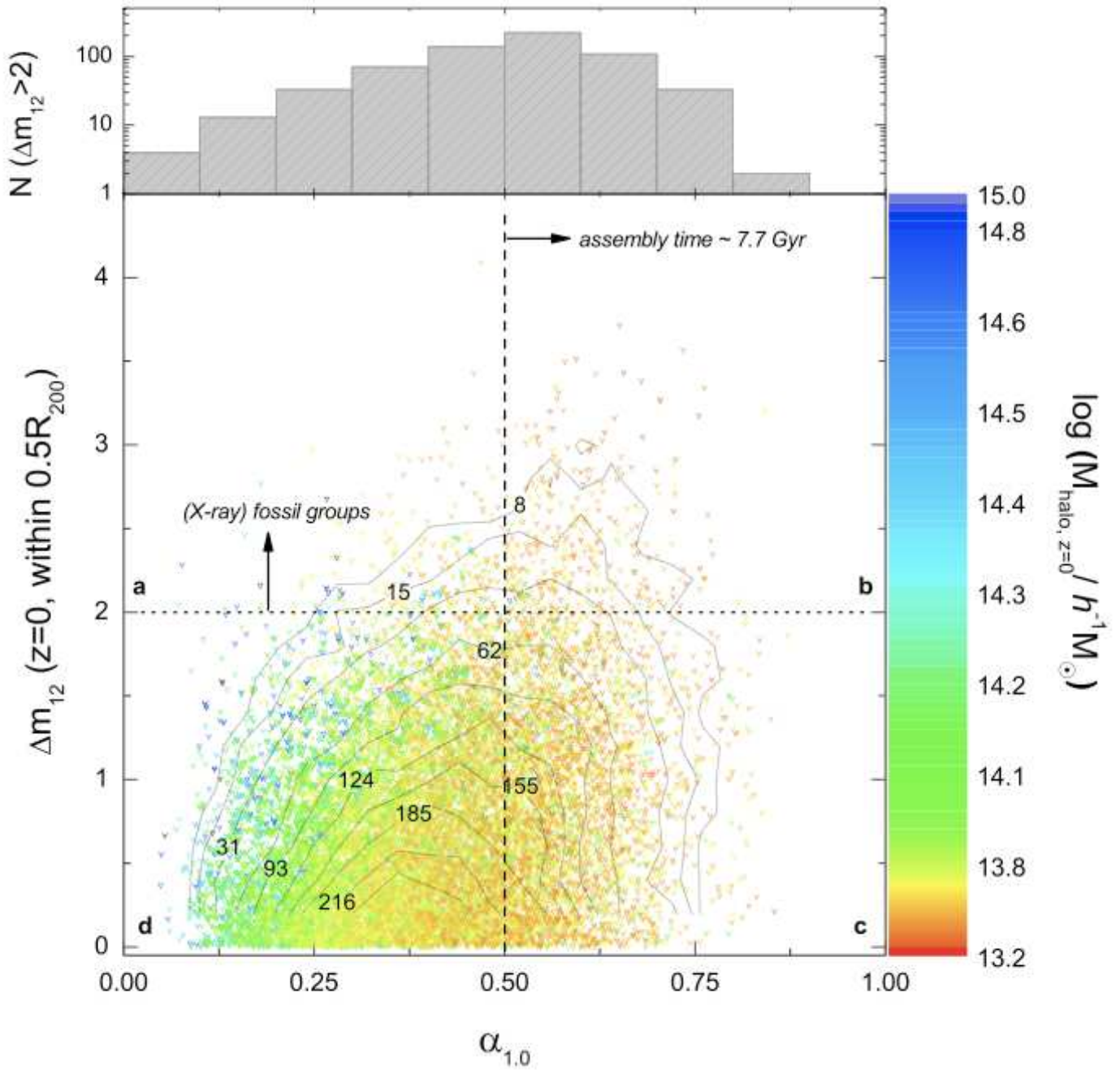


**Figure 3.** The magnitude gap  $\Delta m_{12}$  within  $0.5 R_{200}$ , estimated for all 14628 X-ray bright groups in Fig. 1 (i.e. groups with  $L_{X,\text{bol}} \geq 0.25 \times 10^{42} h^{-2} \text{erg s}^{-1}$ ) at  $z = 0$  versus the ratio of the group halo mass at redshift  $z = 1$  to its mass at  $z = 0$  ( $\alpha_{1,0}$ ). The horizontal dashed-line separates groups into fossils ( $\Delta m_{12} \geq 2.0$ ) and non-fossils ( $\Delta m_{12} < 2.0$ ). The vertical dashed-line corresponds to  $\alpha_{1,0} = 0.5$ . Groups with  $\alpha_{1,0} \geq 0.5$  have formed more than half of their mass by  $z \sim 1.0$  and hence have a minimum assembly time of about  $\sim 7.7$  Gyr. Data points are colour-coded according to FoF group halo mass  $M_{R200}$  at present epoch. The density of data points is represented by black contour lines which is the number of groups in each of  $25 \times 25$  cells of an overlaid grid, equally spaced horizontally and vertically. The upper panel represents the histogram of X-ray bright fossil groups, i.e. all groups with  $\Delta m_{12} \geq 2.0$  and  $L_{X,\text{bol}} \geq 0.25 \times 10^{42} h^{-2} \text{erg s}^{-1}$ .

fect class of fossils, though they develop a magnitude gap  $\Delta m_{12}$  which is not as large as those seen in X-ray fossils (see also Figs. 4b1, ..., b6).

On the other hand, unlike old groups, X-ray fossils develop large magnitude gaps, which do not necessarily correspond to their rapid mass growth, especially in massive groups with  $\log(M(R_{200})/h^{-1} M_{\odot}) \geq 14.0$ . This reflects the fact that the ma-

jority of real passive groups have a small magnitude gap between their two brightest galaxies. Thus the expression  $\Delta m_{12} \geq 2$  only partially separates genuine old/passive groups from young/forming groups, as there are a larger fraction of genuine old groups but with small  $\Delta m_{12}$ .

From Figs. 4c4, c5, c6, it is obvious that older groups are essentially more relaxed systems, which have not recently experi-

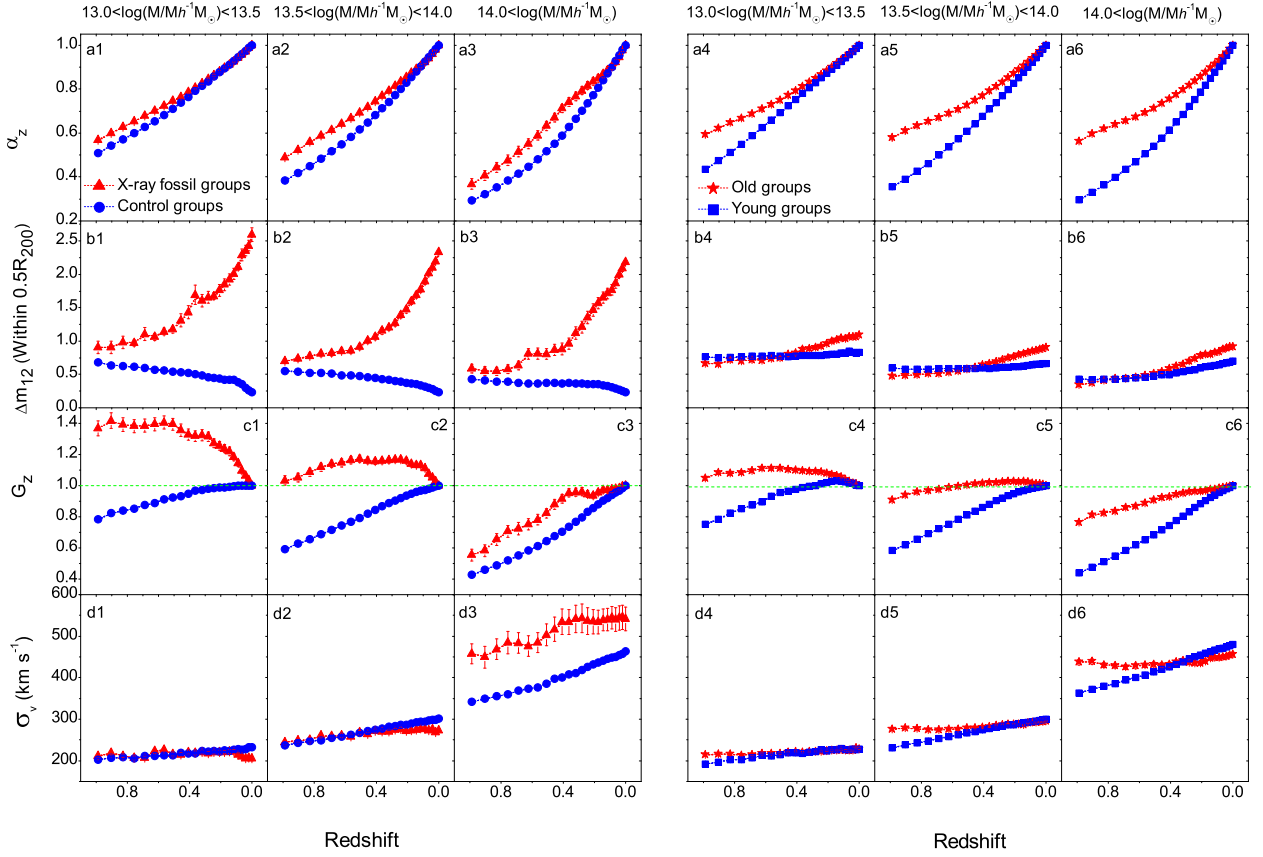


**Figure 4.** The evolution with redshift of various physical parameters of X-ray bright groups, in various ranges of group mass. *Left panel:* Haloes are classified as **X-ray fossil** ( $\Delta m_{12} \geq 2.0$ , red triangles) and **control** ( $\Delta m_{12} \leq 0.5$ , blue circles) groups based on the magnitude gap between the first and the second brightest galaxies within  $0.5R_{200}$ . *Right panel:* Groups are divided into **old** ( $\alpha_{1.0} \geq 0.5$ , red stars) and **young** ( $\alpha_{1.0} \leq 0.5$ , blue squares) population respectively. Each row represents the evolution of a parameter characteristic of galaxy groups that can be measured from the simulations (but not necessarily from observations). From top to bottom the parameters on the y-axis represent: (i)  $\alpha_z$ , the ratio of the group halo mass at redshift  $z$  to its mass at  $z = 0$  ( $a1, \dots, a6$ ), (ii)  $\Delta m_{12}$ , i.e. the magnitude gap between the first two brightest group galaxies found within  $0.5R_{200}$  ( $b1, \dots, b6$ ), (iii)  $G_z$ , the ratio of the number of galaxies within  $0.5R_{200}$  at redshift  $z$  of a given galaxy group to the number of galaxies within  $0.5R_{200}$  at redshift  $z = 0$  of the same group ( $c1, \dots, c6$ ), and (iv) the group velocity dispersion  $\sigma_V$  in  $\text{km s}^{-1}$  ( $d1, \dots, d6$ ). In the third panels from top, the horizontal green dashed-lines intersect the y-axis at  $G_z = 1$ .

enced a major merger, as the rate of infall of galaxies is equal or even less than the rate at which galaxies merge with the central group galaxy. Therefore in old groups the parameter  $G_z$  is more or less constant with time, compared to that of the younger groups within the same group mass bin. The situation is a bit different in X-ray fossils with  $\log(M(R_{200})/h^{-1}M_\odot) \leq 14.0$  (Figs. 4d1, d2), since, in these cases, the rate of galaxy merging is noticeably larger than that of the infall of galaxies. As a result, very large magnitude gaps can develop in X-ray fossil groups. It is also evident both massive X-ray fossils and control groups with  $\log(M(R_{200})/h^{-1}M_\odot) \geq 14.0$  (Fig. 4d3) are in a state of rapid mass growth. As a consequence, massive X-ray groups are not dynamically relaxed systems as they are influenced by infall of galaxies and substructures.

Finally, it is worth considering how the velocity dispersion, plotted in Figs. 4d1, ..., d6 changes with time in the different kinds of groups. As Figs. 4d4, d5, d6 show, as long as the rate of infall of subgroups is close to 1.0 (green dashed-line), the velocity dispersion does not significantly change with time, which in turn is a sign that these groups are certainly relaxed systems.

### 4.2.3 BCG magnitudes

Since the central galaxy in a fossil group is a product of numerous mergers, many of them with luminosities close to  $L_*$  galaxies, X-ray fossils are expected to be dominated by optically luminous brightest galaxies (BCGs) more often than their non-fossil counter-



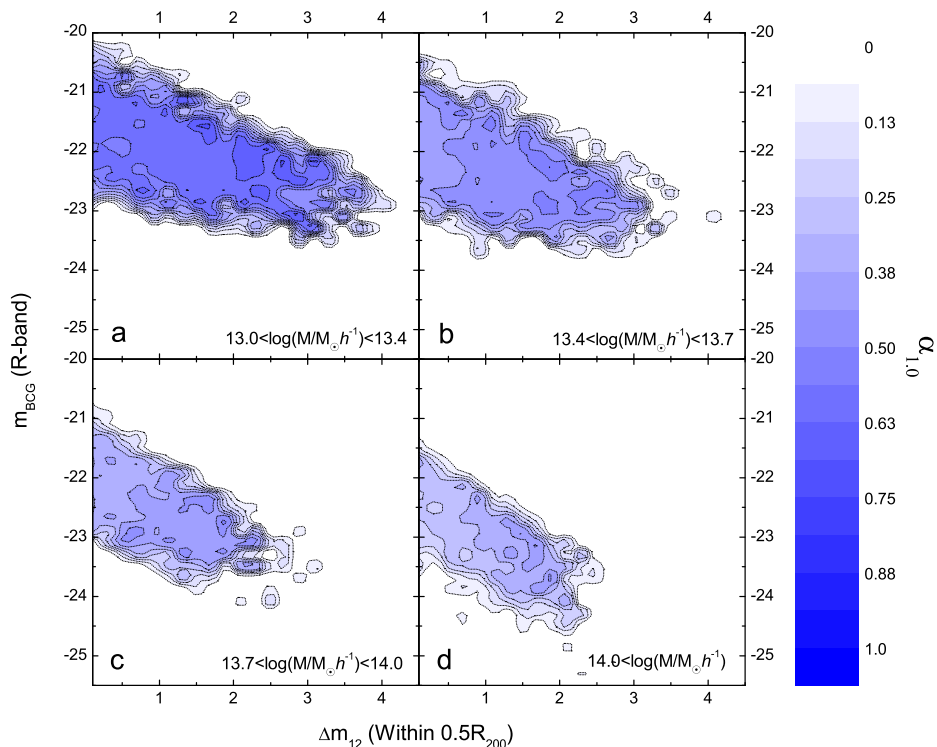


**Figure 5.** The absolute R-band magnitude of BCGs for all X-ray bright groups versus  $\Delta m_{12}$  within  $0.5R_{200}$  in four different mass bins. A grid of  $45 \times 55$  cells has been superposed in each panel, and the cell is colour-coded according to the median value of  $\alpha_{1,0}$  within the cell. The contours trace the distribution of median  $\alpha_{1,0}$  values in each panel. All panels have the same scale.

parts. Here we explore the correlation between the luminosity of the central galaxies of groups with large magnitude gaps, and their mass assembly history.

The four panels in Fig. 5 demonstrate the relation between the absolute  $R$ -band magnitude of the BCGs for all X-ray bright groups and the magnitude gap  $\Delta m_{12}$  within  $0.5R_{200}$  in four different mass bins. In each panel of Fig. 5, a grid of  $45 \times 55$  cells is overlaid, where each cell is colour-coded according to the median of  $\alpha_{1,0}$  in that cell. Accordingly, contours in each panel trace the distribution of median  $\alpha_{1,0}$  values.

Fig. 5 shows clearly that both  $\alpha_{1,0}$  and BCG  $R$ -band magnitudes increase with decrease in group halo masses. But it does not show a tight correlation between the  $R$ -band luminosity of BCGs and group magnitude gaps  $\Delta m_{12}$ , though the correlation is more pronounced in clusters with  $M(R_{200}) \geq 10^{14} h^{-1} M_{\odot}$  (Fig. 5d). Therefore, imposing a magnitude cut for the BCGs would result in the loss from the sample of a large number of genuine groups which are not X-ray fossil systems according to the optical condition involving  $\Delta m_{12}$ .

### 4.3 The Fossil phase in the life of groups

The existence of large magnitude gaps in X-ray fossils in Figs. 4b1, b2, b3 is expected as these groups were initially selected according to their  $\Delta m_{12}$  at  $z=0$ . It would be interesting if they could be shown to have maintained such large magnitude gaps for

a longer time, in comparison to control groups, which would be the case if X-ray fossils were relaxed groups without recent major mergers. Also if fossil groups in general are the end results of galaxy merging, then we do expect the majority of fossils selected at higher redshifts to still be detected as fossils at the present epoch. In other words, the *fossil phase* in the life of a galaxy group should be long-lasting.

To test this, we select three sets of fossil groups with  $\Delta m_{12} \geq 2.0$  at three different redshifts. By tracing the magnitude gap of each set from  $z=1.0$  to  $z=0$ , we examine the fossil phase of each set in time. In Fig. 6, fossils (*black shaded histogram*) and control (*black thick line histogram*) groups are selected at  $z=0$  (*left column*),  $z=0.4$  (*middle column*), and  $z=1.0$  (*right column*). Fractions of fossil and control groups in each column of Fig. 6 have been separately estimated by normalising the number of fossil and control groups at other redshifts to their total numbers at the redshift at which they were initially selected.

This plot shows that, contrary to expectation, no matter at what redshift the fossils are selected, after  $\sim 4$  Gyr, more than  $\sim 90\%$  of them change their status and become non-fossils according to the magnitude gap criterion. Over the span of 7.7 Gyr, which is the time interval between  $z=0-1$ , very few groups retain a two-magnitude gap between the two brightest galaxies. This means that the fossil-phase is a temporary phase in the life of fossil groups (also see von Benda-Beckmann et al. 2008), and there is no guarantee that an observed fossil group, at a relatively high redshift, remains a

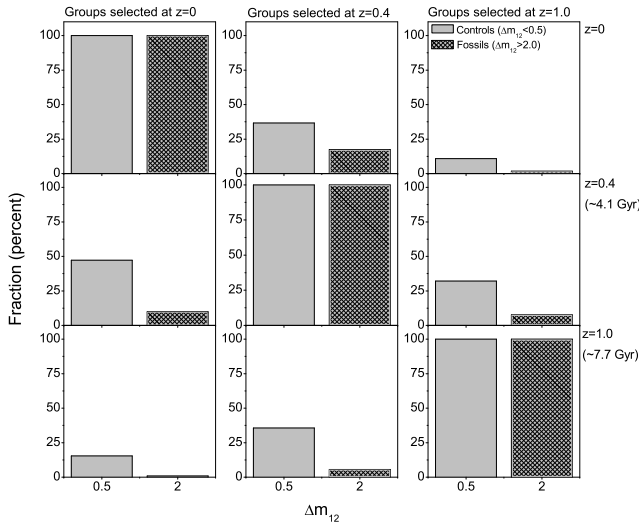


**Figure 6.** The fate of fossil groups identified at different redshifts. Fossil groups (*dark shaded histogram*) and control groups (*grey shaded histogram*) are initially selected at  $z=0$  (*left column*),  $z=0.4$  (*middle column*), and  $z=1.0$  (*right column*). For these objects, we explore what fraction remain “fossil” or “control” groups at two other epochs in the redshift range  $0 \lesssim z \lesssim 1.0$ . It is clear that the fossil phase does not last in  $> 90\%$  of groups after 4 Gyr, no matter at which epoch they are identified.

fossil until the present time, if fossils are selected according to their magnitude gap  $\Delta m_{12} \geq 2.0$ .

## 5 REVISING THE OPTICAL CRITERION FOR FINDING FOSSIL GROUPS

Using the Millennium simulation DM runs as well as the gas and semi-analytic galaxy catalogues based on them, it seems from the above that the conventional optical condition  $\Delta m_{12} \geq 2$ , used to classify groups as fossils, does not ensure that these systems represent a class of old galaxy groups, in which the central galaxy has grown through the merging of other comparable group galaxy members. Having said that, it is true that the magnitude gap in a galaxy group is related to the mass assembly history of the group, for we saw that in groups, such a gap develops gradually with time. However, the difference between the luminosities of the two brightest galaxies in groups is not always reliable for the identification of fossil systems, as this quantity is vulnerable to the assimilation of a comparable galaxy into the core of the group, as a result of infall or merger with another group.

We therefore attempt to identify a more robust criterion, in terms of the difference of optical magnitudes among the brightest galaxies in a group, which might be better suited to identifying systems where most of the mass has been assembled at an early epoch. As introduced in Sec. 4.2.2, we quantify the age of a group in terms of the mass assembly parameter  $\alpha_{1.0}$ , which for an individual group is the ratio of its mass at redshift  $z = 1.0$  to its present mass at  $z = 0$ , i.e.  $\alpha_{1.0} \equiv M_{z=1.0}/M_{z=0}$ . We begin by considering the effect of the radius within which the magnitude gap is calculated.

### 5.1 A general criterion for the magnitude gap

Assume a general optical condition in defining early-formed groups according to the magnitude gap between the brightest group galaxy and other group members in the following form:

$$\Delta m_{1i} \geq j, \quad (1)$$

where  $\Delta m_{1i}$  is the difference in  $R$ -band magnitude between the first brightest group galaxy and the  $i^{\text{th}}$  brightest group galaxy within  $0.5R_{200}$  (or  $R_{200}$ ) of the group centre. The current definition of fossils involves  $i = 2$  and  $j = 2$ . Obviously any group satisfying Eq. 1 must contain at least  $i$  galaxies. We do not consider  $i > 10$  since then we have to exclude most groups in our sample, and it would turn out not be very useful for observers as well.

As we consider the magnitude gap between the brightest to the  $i^{\text{th}}$  ( $=2, 3, \dots, 9, 10$ ) brightest galaxy, the value of the magnitude gap varies from  $j \gtrsim 0$  to  $j \lesssim 5$ . Our aim is to find a pair of  $(i, j)$  in Eq. 1 which yields the best selection of genuinely old groups with a history of early mass assembly.

In Fig. 7, we show how the parameter  $\alpha_{1.0} \equiv M_{z=1.0}/M_{z=0}$ , which represents the mass assembly of groups since redshift  $z=1.0$ , depends upon the selection of  $i$  and  $j$  in Eq. 1. For each value of  $i$  in Fig. 7, groups are first sorted according to their magnitude gaps  $\Delta m_{1i}$  estimated within  $0.5R_{200}$  or  $R_{200}$ , where the latter is the overdensity radius of the group. For each  $i$ , the average value for  $\alpha_{1.0}$  is calculated, for each value of  $j$ , for all groups satisfying Eq. 1. The plot is colour-coded according to the values of  $\alpha_{1.0}$ . The *black contours* give an idea of the number of groups involved: the fraction of the total number of groups identified by parameters  $(i, j)$  is constant along each of these lines.

From Fig. 7a, for instance, we find that systems with  $i = 4$  and  $j = 3$ , i.e. systems for which  $\Delta m_{14} \geq 3$  (within  $0.5R_{200}$ ), yield  $\sim 2.4\%$  of groups with  $\alpha_{1.0} \sim 0.54$ . The same is  $\sim 1.2\%$  with  $\alpha_{1.0} \sim 0.56$ , if one estimates  $\Delta m_{14} \geq 3$  within  $R_{200}$  according to Fig. 7b.

In fact, by changing our search radius from  $0.5R_{200}$  to  $R_{200}$ , we find  $\sim 50\%$  fewer groups satisfying Eq. 1, for the same value of  $\alpha_{1.0}$ . Therefore, hereafter, we just use Panel a of Fig. 7 which estimates the magnitude gap  $\Delta m_{1i}$  within half of the overdensity radius, i.e.  $0.5R_{200}$ . From this plot, the fraction of groups picked out by applying the conventional fossil criterion  $\Delta m_{12} \geq 2$  is  $\sim 4.0\%$  with  $\alpha_{1.0} \sim 0.52$ .

If we were to find an improved criterion for finding fossils, a better set of parameters  $(i, j)$  in Eq. 1 should

- (i) identify groups with larger value of  $\alpha_{1.0}$ , and/or
- (ii) find a larger fraction of groups with the same or larger value of  $\alpha_{1.0}$ ,

than found in conventional fossils, i.e. groups with  $(i, j)=(2, 2)$ .

For example, by choosing  $i = 4$  and  $j = 3$ , the fraction of groups found with  $\Delta m_{14} \geq 3$  turns out to be  $\sim 40\%$  less than when  $i=j=2$ , but it would identify slightly older groups, with an average  $\alpha_{1.0} \sim 0.55$ , whereas the average  $\alpha_{1.0} \sim 0.52$  in fossils with  $i=j=2$ . In other words,  $(i, j)=(4, 3)$  identifies marginally older groups, at the expense of losing a large number of early-formed groups, compared to the case of conventional fossils  $(i, j)=(2, 2)$ .

Exploring Fig. 7a, we adopt  $(i, j)=(4, 2.5)$  as an example of how the fossil search criterion can be improved. If we define all groups with  $\Delta m_{14} \geq 2.5$  within  $0.5R_{200}$  as fossils, then we would find groups with on average the same mass assembly history, i.e. the same average value of  $\alpha_{1.0}$ , but we would identify  $\sim 50\%$

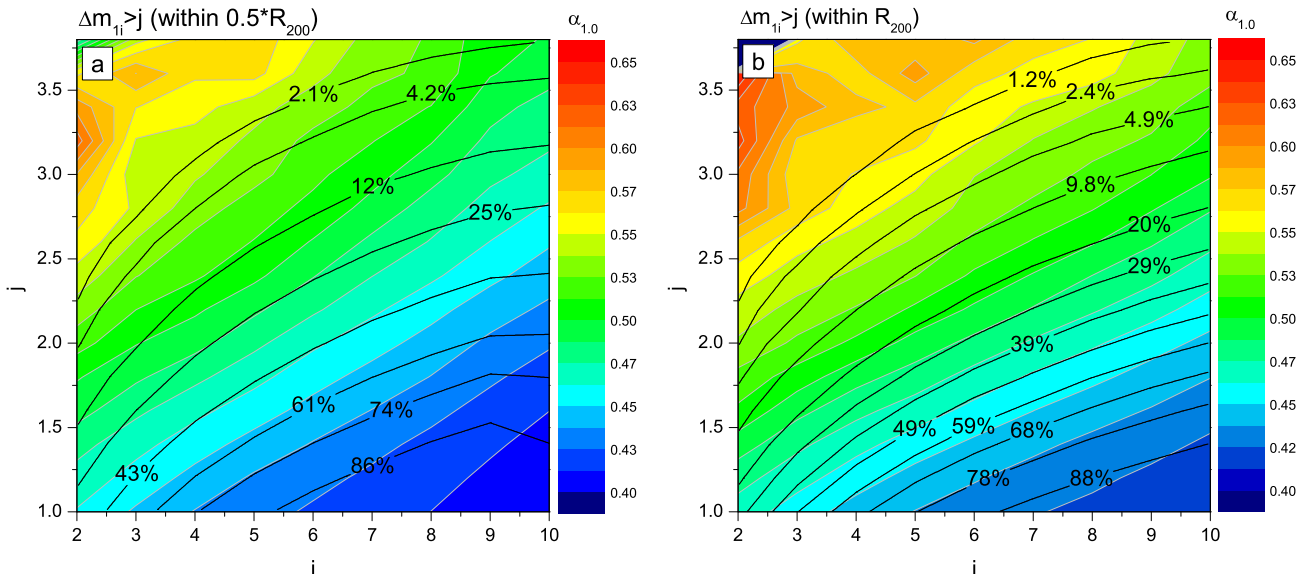


**Figure 7.** The dependence on  $(i, j)$ , defined in Eq. 1, of the mass assembly parameter  $\alpha_{1.0}$ , which is defined as the ratio of the mass of a group at redshift  $z = 1.0$  to its mass at  $z = 0$ , i.e.  $\alpha_{1.0} \equiv M_{z=1.0}/M_{z=0}$ . For each value of  $i$ , groups are sorted according to the value of their magnitude gaps  $\Delta m_{1i}$  calculated within a certain radius (different for the two panels). Then, for different values of  $j$ , the average for  $\alpha_{1.0}$  is calculated for all groups satisfying Eq. 1. The plot is colour-coded according to  $\alpha_{1.0}$ . The *black contours* are drawn such that the fraction of the total number of groups identified is constant along each line. The magnitude gap  $\Delta m_{1i}$  is calculated (**Panel a.**) within half the overdensity radius, i.e.  $0.5R_{200}$ , and (**Panel b.**) within the overdensity radius, i.e.  $R_{200}$ .

more such groups, compared to groups identified the conventional parameters  $(i, j)=(2, 2)$ .

We will examine such groups further in the next section. Meanwhile, the Figs. 7 will allow the user to find their favourite combination of  $(i, j)$  for both  $0.5R_{200}$  and  $R_{200}$ .

## 5.2 The optical criterion $\Delta m_{14} \geq 2.5$ within $0.5R_{200}$

Having explored alternative criteria for identifying groups with a history of early formation, we now compare the history of mass assembly of groups selected according to  $\Delta m_{14} \geq 2.5$  (these groups are hereafter collectively referred to as  $F_{14}$ ) with those groups selected according to  $\Delta m_{12} \geq 2.0$  (hereafter  $F_{12}$ ), both within  $0.5R_{200}$  of the group centre. The latter category are the conventional fossil groups.

The *blue histogram* in Fig. 8 represents the distribution of the mass assembly parameter  $\alpha_{1.0}$  for all X-ray bright groups (as defined in Fig. 1) in our sample. It also shows the groups in the categories  $F_{14}$  (*red thick histogram*) and  $F_{12}$  (*grey shaded histogram*). The *green shaded histogram* corresponds to groups that satisfy both criteria, i.e.  $F_{12} \cap F_{14}$ . The *green dash dotted line* intersects the x-axis at  $\alpha_{1.0} = 0.5$ , representing groups for which half of their mass had been assembled at redshift  $z = 1$ . Gaussian fits to each histogram are overlaid.

Panels **a**, **b**, and **c** in Fig. 8 correspond to different ranges of the logarithm of the group halo mass  $13.0 \leq \log M(R_{200})$ ,  $13.0 \leq \log M(R_{200}) \leq 13.5$ , and  $\log M(R_{200}) \geq 13.5$  respectively, where  $M(R_{200})$  is in units of  $h^{-1} M_{\odot}$ . These figures, as well as the values of the peaks of Gaussian fits to the distribution of  $\alpha_{1.0}$  in each case (given in Table 1) lead to the following observations:

- (i) The groups belonging to  $F_{12}$  and  $F_{14}$  are older than the over-

all population of X-ray bright groups (for all values of halo mass), though such a difference is less pronounced in low-mass systems. Since haloes are thought to be hierarchically assembled, one expects to find a higher incidences of early-formed and low-mass groups in comparison to massive systems.

(ii) Within the errors, groups belonging to  $F_{14}$  are almost as old as  $F_{12}$ , i.e. the estimated  $\alpha_{1.0}$  in  $F_{12}$  systems (as given in Table. 1) is more or less the same as found in  $F_{14}$  systems. However, the fraction of groups in category  $F_{14}$  is at least 50% more than  $F_{12}$ . This tells us that in general, the criterion  $\Delta m_{14} \geq 2.5$  has a higher efficiency of identifying early-formed systems than  $\Delta m_{12} \geq 2.0$ .

(iii) Interestingly,  $\sim 75\%$  of  $F_{12}$  haloes in Fig. 8a also fulfil the  $\Delta m_{14} \geq 2.5$  condition. Conversely,  $\sim 35\%$  of  $F_{14}$  haloes satisfy the  $\Delta m_{12} \geq 2.0$  criterion. This means that a large proportion of the population of early-formed groups in the category  $F_{14}$  is different from those in  $F_{12}$ . Groups which satisfy both criteria, i.e.  $F_{12} \cap F_{14}$ , are not necessarily older in comparison to those belonging to either  $F_{12}$  or  $F_{14}$  (see Table. 1).

(iv) Fig. 8b shows that in fact neither criterion  $\Delta m_{12} \geq 2.0$  nor  $\Delta m_{14} \geq 2.5$  is efficient in finding early-formed groups in low-mass regime, even among X-ray bright groups.

In the following section, we compare the environment and abundance of the groups belonging to the  $F_{12}$  and  $F_{14}$  categories.

## 5.3 The local environment of fossil groups

If galaxy mergers are responsible for the absence of bright galaxies in groups such as X-ray bright fossils, then most of the matter infall into these systems would have happened at a relatively earlier epoch. Consequently, at the present time, old groups should be more isolated than groups which have recently formed (e.g. La Barbera et al. 2009). Here we examine the local environment

**Table 1.** Peak values (from Gaussian fits) of the histograms of the mass assembly parameter  $\alpha_{1.0}$  for various classes of groups. (see Fig. 8). Group halo mass  $M(R_{200})$  is in units of  $h^{-1} M_{\odot}$ .  $F_{14}$  consists of all groups with  $\Delta m_{14} \geq 2.5$ , and  $F_{12}$ , those with  $\Delta m_{12} \geq 2.0$ , both within  $0.5R_{200}$  of the group centre.

Group type	$13.0 \leq \log M(R_{200})$ Panel a	$13.0 \leq \log M(R_{200}) \leq 13.5$ Panel b	$\log M(R_{200}) \geq 13.5$ Panel c
All X-ray bright groups	$0.41 \pm 0.01$	$0.52 \pm 0.01$	$0.38 \pm 0.01$
$F_{12}$	$0.53 \pm 0.01$	$0.56 \pm 0.01$	$0.49 \pm 0.01$
$F_{14}$	$0.52 \pm 0.01$	$0.55 \pm 0.01$	$0.48 \pm 0.01$
$F_{12} \cap F_{14}$	$0.54 \pm 0.01$	$0.55 \pm 0.01$	$0.50 \pm 0.02$

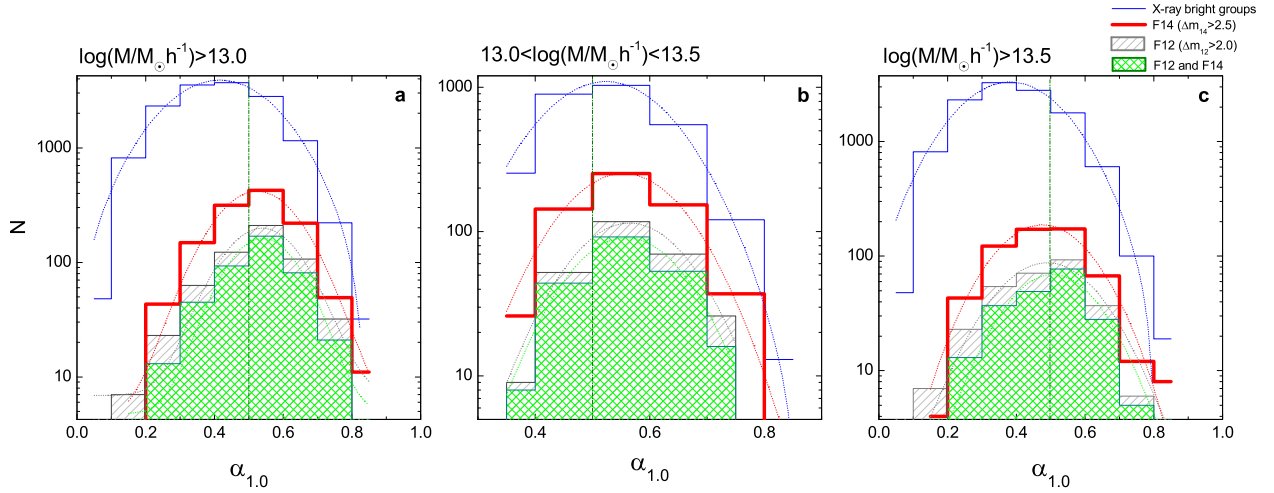


**Figure 8.** Histograms of the mass assembly parameter  $\alpha_{1.0}$  for X-ray bright groups (*blue histogram*), groups that satisfy the criterion  $F_{14}$  (*red thick histogram*), those that satisfy  $F_{12}$  (*gray shaded histogram*), and groups that satisfy both criteria, i.e.  $F_{12} \cap F_{14}$  (*green shaded histogram*). Overlaid are Gaussian fits to each histogram (see Table 1). Panels **a**, **b**, and **c** correspond to the logarithm of the group halo mass in the range  $13.0 \leq \log M(R_{200})$ ,  $13.0 \leq \log M(R_{200}) \leq 13.5$ , and  $\log M(R_{200}) \geq 13.5$  respectively, the unit of  $M(R_{200})$  being  $h^{-1} M_{\odot}$ . The *green dash dotted line* intersects the  $x$ -axis at  $\alpha_{1.0} = 0.5$  where haloes have assembled 50% of their mass at redshift  $z=1.0$ .

of groups, using the density parameter  $\Delta_4$ , defined as the number of haloes within a distance of  $4 h^{-1}$  Mpc from the centre of each group. The local densities are calculated at  $z = 0$  according to

$$\Delta_4 = \frac{\rho_4}{\rho_{bg}} - 1, \quad (2)$$

where  $\rho_4$  is the number density of haloes within a spherical volume of  $4 h^{-1}$  Mpc in radius, and  $\rho_{bg}$  is the background density of haloes within the whole volume of the Millennium simulation. Since the mass assembly of groups is mostly influenced by the infall of subgroups, which individually have masses typically below  $\sim 10\%$  (and often substantially smaller) of the parent halo mass, it is important to take into account all haloes with  $M(R_{200}) \geq 10^{11} h^{-1} M_{\odot}$  from the FoF group catalogue in order to estimate  $\Delta_4$ .

From Gaussian fits to the histograms of the local density  $\Delta_4$  of  $F_{12}$  and  $F_{14}$ , control groups, as well as those of all X-ray bright groups, we find

$$\Delta_4 = \begin{cases} 6.31 \pm 0.17 & \text{for Control groups } (\Delta m_{12} \leq 0.5) \\ 6.25 \pm 0.18 & \text{for X-ray bright groups} \\ 5.10 \pm 0.35 & \text{for } F_{12} \\ 5.19 \pm 0.26 & \text{for } F_{14} \end{cases} \quad (3)$$

where  $\Delta_4$  is estimated using Eq. 2. It seems that both  $F_{12}$  and  $F_{14}$  groups are more likely to lie in lower density regions than control groups and X-ray bright groups. This is in agreement with our expectation as early-formed groups are assumed to be in low-density local environments. However, the local density around  $F_{12}$  and  $F_{14}$  groups is more or less the same. This is consistent with the fact that  $F_{12}$  and  $F_{14}$  have similar values of  $\alpha_{1.0}$  (see Table 1).

A similar trend is seen for density measures  $\Delta_5$  and  $\Delta_6$ , but as the sampling volume increases ( $> \Delta_6$ ), the above trend disappears, showing that the trend is related to the immediate environment of groups.

#### 5.4 The abundance of fossil groups

Various studies have shown that the fraction of early-formed groups increases as the group halo mass decreases (e.g. Milosavljević et al. 2006; Dariush et al. 2007). This phenomenon reflects the fact that structures form hierarchically, where small virialised groups form early, whereas most massive clusters form late. As the merging of galaxies in clusters is less efficient than in groups, due to the high velocity dispersion of cluster galaxies, clusters are less likely to develop large magnitude gaps. At the same time, in low-mass groups (see, e.g., Miles et al. 2004, 2006) dynamical friction is more effective in ensuring galaxies fall to the core of the system, due to the smaller relative velocities involved. As a result, the existence of large magnitude gaps should be more frequently found in groups than in clusters. Thus, to find an old population of groups according to some criterion, and to study the way the criterion depends on group halo mass, would be a good test for the validity of the condition.

The *top panel* of Fig. 9 displays the abundance of  $F_{12}$  (gray shaded histogram) and  $F_{14}$  (red thick line) groups, defined as the fraction of haloes in each category, as a function of halo mass. The range of halo mass explored is  $\log M(R_{200}) \gtrsim 13.4$  in units of  $h^{-1} M_{\odot}$ . Below this mass limit, the number of groups abruptly decrease, since all groups here have been chosen to be X-ray bright groups (see Fig. 1).

The plot shows that in comparison to the  $F_{12}$  groups, the  $F_{14}$  groups are populated by less massive haloes. This can be better seen in the *bottom panel* of Fig. 9, where the relative fraction of  $F_{14}$  groups over  $F_{12}$  is shown. It can be inferred that, on average, the fraction of  $F_{14}$  groups with halo mass  $M(R_{200}) \leq 10^{14} h^{-1} M_{\odot}$  is at least 50% more than the fraction of  $F_{12}$ . However, in the mass range  $M(R_{200}) \geq 10^{14} h^{-1} M_{\odot}$ , the fraction of  $F_{14}$  groups decreases, though since the overall numbers in the extremely high mass range are low, the statistics are poorer.

#### 5.5 The survival of the magnitude gap: $F_{12}$ vs. $F_{14}$

In Sec. 4.3, it was found that, in general, for the conventional fossil groups ( $F_{12}$ ), the *fossil phase* is transient,  $\gtrsim 90\%$  of such groups ceasing to remain fossils after 4 Gyr. Here we examine whether the fossil phase in  $F_{14}$  groups fares better.

The histograms in Fig. 10 represent the fractions of  $F_{12}$  (black line) and  $F_{14}$  (thick red line), as a function of look-back time in Gyr. The plot shows that in comparison to the  $F_{12}$  groups, the *fossil phase* lasts longer by almost 1 Gyr for the same fraction of  $F_{14}$  groups. For example, the fraction of  $F_{12}$  groups that maintains its magnitude gap after  $\sim 2.2$  Gyr, falls to 28%, while the corresponding period is  $\sim 3.2$  Gyr in  $F_{14}$ . Thus, not only does the  $\Delta m_{14} \geq 2.5$  condition identify at least 1.5 times as many fossil groups as the  $F_{12}$  condition, it also identifies groups in which the fossil phase lasts significantly longer. This can be explained from our analysis of the halo mass distribution within  $F_{12}$  and  $F_{14}$ , already discussed in Sec. 5.4.

#### 5.6 Comparison with observed groups

When making detailed comparisons between simulations and catalogues of galaxies and groups compiled from observations, one has to be aware that simulated dark matter haloes have limited resolution, as mentioned in § 2.2.1 and 2.2.2. This means that all galaxies in the semi-analytic models, assigned to a particular halo, might not belong to dark matter subhalos. We find that even after applying a

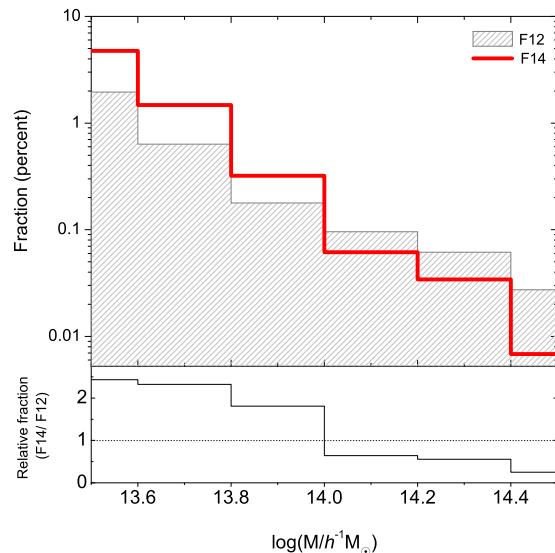


**Figure 9. Top panel:** The abundance of  $F_{12}$  (gray shaded histogram) and  $F_{14}$  (red thick line) groups, i.e., the fraction of groups in each category as a function of halo mass. **Bottom panel:** The relative fraction of  $F_{14}$  over  $F_{12}$  groups as a function of halo mass.

magnitude cut, there would be a significant number of modelled galaxies, whose orbits are analytically calculated, that would end up being not a member of a sub-halo, and thus would not be classified as a group member.

While dealing with magnitude gaps  $\Delta m_{12}$  and  $\Delta m_{14}$ , it is worth examining to what extent these quantities are vulnerable to resolution effects like the above. A direct way would be to compare the magnitude gap distribution of groups, selected based on their  $\Delta m_{14}$ , between simulations and observations. This is not a straightforward task, as groups identified from observational sky surveys are biased due to incompleteness in measured magnitude and redshift. Furthermore, a variety of group finding algorithms are adopted to identify groups in simulations and observation, which adds uncertainties to any such comparison.

Here, we use the group catalogue of Yang et al. (2007), which uses a halo-based group finder on the Sloan Digital Sky Survey (SDSS DR4). They define groups as systems whose dark matter haloes, have an overdensity of 180, determined from dynamics. This makes this catalogue suitable for comparison with the Millennium simulation, where dark matter halos have an overdensity of 200. From Sample II of the catalogue, groups with following properties are selected:

- they have at least four members,
- they are within the redshift range  $0.01 \leq z \leq 0.1$ , and
- their estimated halo mass is  $\log M(R_{180}) \geq 13.25, h^{-1} M_{\odot}$ ,

since our Millennium X-ray groups have a similar mass threshold (see Fig. 1).

After applying the above criteria, 1697 groups were identified, and their magnitude gaps were compared with galaxy groups selected from the Millennium simulation at redshift  $z \sim 0.041$ . The magnitude gap distributions from both SDSS-DR4 as well as the Millennium simulation are shown in Fig. 11. Panels **a** and **b** of

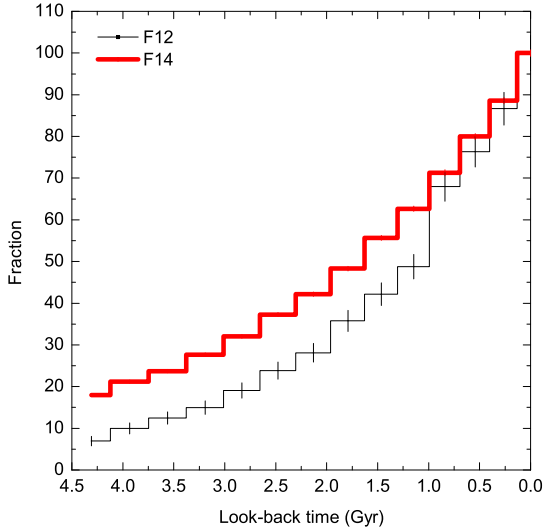


**Figure 10.** The fractions of F<sub>12</sub> (black line) and F<sub>14</sub> (thick red line) groups, identified at redshift  $z=0$ , that survive as fossils, as a function of look-back time.

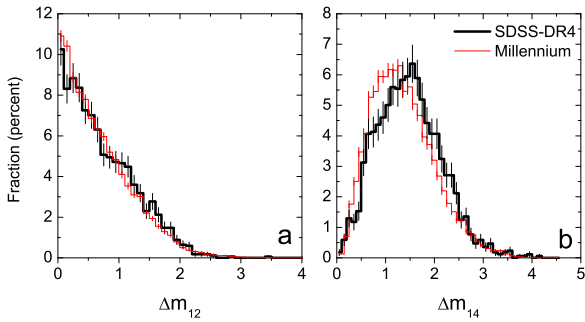


**Figure 11.** The  $R$ -band magnitude gap distribution for haloes from the Millennium semi-analytic models of Bower et al. (2006) (red histograms) superposed on the  $r$ -band data from Sample II of SDSS-DR4 group catalogue of Yang et al. (2007) (black histograms). (a) This shows the magnitude gap  $\Delta m_{12}$  between the first and second most luminous galaxies, compared with galaxies from the SDSS-DR4 catalogue of groups computed within group radius. (b) This is the same as in (a), but for the magnitude gap  $\Delta m_{14}$  between the first and the fourth most luminous galaxies. The 1697 SDSS-DR4 groups are within the mass range  $\log(M(R_{180})/h^{-1} M_{\odot}) \geq 13.25$ , and redshift range  $0.01 \leq z \leq 0.1$ . Those from the Millennium simulations consist of 14612 X-ray groups selected at redshift  $z \sim 0.04$  in the same mass range.

Fig. 11 refer to the magnitude gap distribution  $\Delta m_{12}$  and  $\Delta m_{14}$  respectively. Results show that the estimated magnitude gaps are in fair agreement with observation. The fraction of groups with  $\Delta m_{12} \geq 2.0$  is more or less the same while the fraction of those galaxy groups with  $\Delta m_{14} \geq 2.5$  is different by  $\sim 1\%$  (see Table. 2). This shows that the incompleteness resulting from limited resolution does not affect our statistics.

**Table 2.** Comparison between the observed and simulated fraction of groups with magnitude gaps  $\Delta m_{12}$  and  $\Delta m_{14}$ , estimated from the histograms presented in Fig. 11.

Selection criterion	SDSS (DR4) (Yang et al. 2007)	Millennium simulation (Bower et al. 2006)
$\Delta m_{12} \geq 2.0$	$2.0\% \pm 0.4$	$2.1\% \pm 0.2$
$\Delta m_{14} \geq 2.5$	$6.2\% \pm 0.6$	$5.1\% \pm 0.2$

## 6 DISCUSSION AND CONCLUSIONS

In this work, we analysed the evolution of the magnitude gap (the difference in magnitude of the brightest and the  $n$ th brightest galaxies) in galaxy groups. Using the Millennium dark matter simulations and associated semi-analytical galaxy catalogues and gas simulations, we investigated how the magnitude gap statistics are related to the history of mass assembly of the group, assessing whether its use as an age indicator is justified.

A catalogue of galaxy groups, compiled from the Millennium dark matter simulations, was cross-correlated with catalogues resulting from hot gas simulations, and from semi-analytic galaxy evolution models based on these simulations. This resulted in a list of groups, with various properties of the associated dark matter haloes and galaxies, at 21 time steps, over the redshift range  $z \simeq 1.0$  to  $z=0$ . The simulated X-ray emitting hot IGM properties were known for these haloes only for  $z=0$ , and these were used to define a sample of X-ray emitting groups. This is necessary since our objective was to examine the evolution of fossil groups, which are observationally defined in terms of both optical and X-ray parameters.

We compared the estimated magnitude gaps in these galaxy groups from two different semi-analytic models of Bower et al. (2006) and Croton et al. (2006), based on the Millennium dark matter simulations, and found that the model of Bower et al. (2006) better matches the observed present-day distribution of the difference in magnitude between the brightest galaxy in each group, and the second and third brightest galaxies  $\Delta m_{12}$  and  $\Delta m_{13}$ . We decided to use the Bower et al. (2006) catalogue for the rest of this study.

We examined the evolution with time of fossil galaxy groups, conventionally defined as those with an  $R$ -band difference in magnitude between the two brightest galaxies  $\Delta m_{12} \geq 2$  (within  $0.5 R_{200}$  of the group centre). We explored the nature of the groups that would be selected if the radius of the group were extended to  $R_{200}$ , and the definition of the magnitude gap in terms of  $\Delta m_{1i}$  were varied. Our major conclusions from the analyses can be summarised as follows:

(i) The parameter  $\Delta m_{1i}$  defined for a galaxy system as the magnitude gap between the first and  $i^{\text{th}}$  brightest galaxies (estimated within a radius of  $0.5R_{200}$  or  $R_{200}$ ) can be shown to be linked to the halo mass assembly of the system  $\alpha_{1,0}$  (Fig. 7), such that *galaxy systems with larger magnitude gaps  $\Delta m_{1i}$  are more likely to be early-formed than those with smaller magnitude gaps.*

(ii) Fig. 6 shows that, contrary to expectation, irrespective of the redshift at which fossil groups are identified according to the usual criteria, after  $\sim 4$  Gyr, more than  $\sim 90\%$  of them become non-fossils according to the magnitude gap criterion. Over the span of 7.7 Gyr, which is the time interval between  $z=0-1$ , very few groups retain a two-magnitude gap between the two brightest galaxies. This pro-

vides clear evidence that the fossil phase is a temporary phase in the life of fossil groups (also see von Benda-Beckmann et al. 2008).

(iii) In a given galaxy group, the merging of the  $i^{\text{th}}$  brightest (or a brighter) galaxy, with the brightest galaxy in the group (often the central galaxy if there is one), results in an increase of  $\Delta m_{1i}$ . However, one of the main reasons for the fossil phase to be a transient one is that such a magnitude gap could be filled by the infall of equally massive galaxies into the core of the group, which would lead to a decrease in  $\Delta m_{1i}$ . Therefore, groups with smaller magnitude gaps are not necessarily late-formed systems. Many groups spend a part of their life in such a fossil phase, though an overwhelming majority of them would not fulfil the criteria of the “fossil” label at all epochs.

(iv) For our sample of X-ray bright groups, the optical criterion  $\Delta m_{14} \geq 2.5$  in the  $R$ -band is more efficient in identifying early-formed groups than the condition  $\Delta m_{12} \geq 2.0$  (for the same filter), and is shown to identify at least 50% more early-formed groups. Furthermore, for the groups selected by the latter criterion, the *fossil phase* in general is seen on average to last  $\sim 1.0$  Gyr more than their counterparts selected using the conventional criterion.

(v) Groups selected according to  $\Delta m_{14} \geq 2.5$  at  $z = 0$  correspond to  $\sim 75\%$  of those identified using the  $\Delta m_{12} \geq 2.0$  criterion. On comparing different panels in Fig. 8, one finds that early-formed groups identified from their large magnitude gaps (either  $\Delta m_{12} \geq 2.0$  or  $\Delta m_{14} \geq 2.5$ ) represent a small fraction (18% for F14 and 8% for F12) of the overall population of early-formed systems. This is especially noticeable in the high-mass regime.

(vi) Finally, Fig. 9 shows that in comparison to conventional fossils (i.e. F<sub>12</sub> groups), the F<sub>14</sub> groups identified based on  $\Delta m_{14} \geq 2.5$ , predominantly correspond to systems with halo masses  $M(R_{200}) \leq 10^{14} h^{-1} M_{\odot}$ .

This makes the criterion  $\Delta m_{12} \geq 2.0$  marginally more efficient than  $\Delta m_{14} \geq 2.5$  in identifying massive early-formed systems.

These results depend to some extent on the employed semi-analytic model in our current analysis, and the statistics might change if one uses different semi-analytical model of galaxy formation.

Physical prescriptions such as galaxy merging, supernova and AGN feedback used in such models are somewhat different from one another. Furthermore, superfluous mergers may result from the algorithm used for the identification of haloes in the Millennium DM simulation, and this may affect the merger rates calculated from various studies, including ours, using these catalogues (e.g. Genel et al. 2009). Though merging is the most important process affecting galaxies in groups, there are other physical processes such as ram pressure stripping, interactions and harassment, group tidal field, and gas loss, that are not fully characterised by current semi-analytic models.

This is partially due to the limited spatial resolution of the Millennium simulation. The new release of the current simulation, i.e. Millennium-II Simulation might help to address some of the above issues. The latter has 5 times better spatial resolution and 125 times better mass resolution (Boylan-Kolchin et al. 2009). Future semi-analytic models based upon high resolution simulations, incorporating such effects would be worth employing in a similar investigation to find better observational indicators of the ages of galaxy groups and clusters.

## ACKNOWLEDGMENTS

The Millennium Simulations used in this paper was carried out by the Virgo Supercomputing Consortium at the Computing Center of the Max-Planck Society in Garching. The semi-analytic galaxy catalogues used in this study are publicly available at <http://galaxy-catalogue.dur.ac.uk:8080/MyMillennium/>. The Millennium Gas Simulations were carried out at the Nottingham HPC facility, as was much of the analysis required by this work. The SDSS-DR4 group catalogue of Yang et al. (2007) used in this study is publicly available at <http://www.astro.umass.edu/~xhyang/Group.html>.

AAD gratefully acknowledges Graham Smith, Malcolm Bremer and the anonymous referee for helpful discussions. The 2dFGRS group catalogue data (Yang et al. 2005, 2007) used in this study was kindly provided by Frank C. van den Bosch and X. Yang.

## REFERENCES

- Bai, L., Rasmussen, J., Mulchaey, J.S., Dariush, A., Raychaudhury, S., Ponman, T.J., 2010, ApJ, submitted
- Balogh, M.L., McCarthy, I.G., Bower, R.G., Eke, V.R., 2008, MNRAS, 385, 1003
- Barnes, J.E., 1989, Nature, 338, 123
- Baugh C. M., 2006, RPPH, 69, 3101
- Borgani S., et al., 2006, MNRAS, 367, 1641
- Bower, R.G. et al., 2006, MNRAS, 370, 645
- Boylan-Kolchin, M., Ma, C.-P., Quataert, E., 2008, MNRAS, 383, 93
- Boylan-Kolchin, M., Springel, V., White, S.D.M., Jenkins, A., Lemson, G., 2009, MNRAS, 398, 1150
- Cole, S.M. et al., 2000, MNRAS, 319, 168
- Croton, D.J., Springel, V., White, S.D.M., De Lucia, G.; Frenk, C. S.; Gao, L.; Jenkins, A., Kauffmann, G., Navarro, J. F. & Yoshida, N., 2006, MNRAS, 365, 11
- Dariush, A., Khosroshahi, H.G., Ponman, T.J., Pearce, F., Raychaudhury, S., Hartley, W., 2007, MNRAS, 382, 433
- Díaz-Giménez E., Muriel H., Mendes de Oliveira C., 2008, A&A, 490, 965
- D’Onghia E., Sommer-Larsen J., Romeo A. D., Burkert A., Pedersen K., Portinari L., Rasmussen J., 2005, ApJ, 630, L109
- Eigenthaler P., Zeilinger W. W., 2009, AN, 330, 978
- Forbes D. A., et al., 2006, PASA, 23, 38
- Genel S., Genzel R., Bouché N., Naab T., Sternberg A., 2009, ApJ, 701, 2002
- Harker, G., et al., 2006, MNRAS, 367, 1039
- Hartley W. G., Gazzola L., Pearce F. R., Kay S. T., Thomas P. A., 2008, MNRAS, 386, 2015
- Jetha N. N., Hardcastle M. J., Babul A., O’Sullivan E., Ponman T. J., Raychaudhury S., Vrtilik J., 2008, MNRAS, 384, 1344
- Jetha N. N., Khosroshahi H., Raychaudhury S., Sengupta C., Hardcastle M., 2009, arXiv, arXiv:0909.0221
- Jones, L.R. et al., 2003, MNRAS, 343, 627
- Khosroshahi H. G., Jones L. R., Ponman T. J., 2004, MNRAS, 349, 1240
- Khosroshahi H. G., Raychaudhury S., Ponman T. J., Miles T. A., Forbes D. A., 2004, MNRAS, 349, 527
- Khosroshahi H. G., Ponman T. J., Jones L. R., 2006, MNRAS, 372, L68
- Khosroshahi, H.G., Ponman, T.J., Jones, L.R., 2007, MNRAS, 377, 595

- La Barbera F., de Carvalho R. R., de la Rosa I. G., Sorrentino G., Gal R. R., Kohl-Moreira J. L., 2009, *AJ*, 137, 3942
- Mahajan S., Raychaudhury S., 2009, *MNRAS*, 400, 687
- Malbon, R.K., et al., 2007, *MNRAS*, 382, 1394
- Miles T. A., Raychaudhury S., Forbes D. A., Goudfrooij P., Ponman T. J., Kozhurina-Platais V., 2004, *MNRAS*, 355, 785
- Miles T. A., Raychaudhury S., Russell P. A., 2006, *MNRAS*, 373, 1461
- Miller, C.J. et al., 2005, *AJ*, 130, 968
- Milosavljević, M., Miller, C.J., Furlanetto, S.R. & Cooray, A., 2006, *ApJ*, 637, L9
- Nolan L. A., Raychaudhury S., Kabán A., 2007, *MNRAS*, 375, 381
- Ponman, T.J., Allan, D.J., Jones, L.R., Merrifield, M. & MacHardy, I.M., 1994 *Nature*, 369, 462
- Rasmussen, J., Ponman, T.J., Mulchaey, J.S., Miles, T.A. & Raychaudhury, S., 2006, *MNRAS*, 373, 653
- Sales, L.V., Navarro, J.F., Lambas, D.G., White, S.D.M. & Croton, D.J., 2007, *MNRAS*, 382, 1901
- Santos, W.A., Mendes de Oliveira, C., & Sodr e, L., 2007, *AJ*, 134, 1551
- Smith, G.P., Khosroshahi, H.G., Dariush, A., Sanderson, A.J.R., Ponman, T.J., Stott, J.P. et al., 2009, *MNRAS*, submitted
- Spergel, D.N. et al., 2003, *ApJS*, 148, 175
- Springel, V., White, S.D.M., Tormen, G. & Kauffmann, G., 2001, *MNRAS*, 328, 726
- Springel, V. et al., 2005, *Nature*, 435, 629
- Steinmetz, M., & White, S.D.M., 1997, *MNRAS*, 288, 545
- van den Bosch, F.C. et al., 2007, *MNRAS*, 376, 841
- Voevodkin A., Borozdin K., Heitmann K., Habib S., Vikhlinin A., Mescheryakov A., Hornstrup A., Burenin R., 2010, *ApJ*, 708, 1376
- von Benda-Beckmann A.M., D’Onghia E., Gottl ber S., Hoefl M., Khalatyan A., Klypin A., M ller V., 2008, *MNRAS*, 386, 2345
- Yang X. H., Mo H. J., van den Bosch F. C., Jing Y. P., 2005, *MNRAS*, 356, 1293
- Yang X. H., Mo H. J., van den Bosch F. C., Pasquali, A., Li, Ch., Barden, M., 2007, *ApJ*, 671, 153